



UNIVERSIDAD DE CUENCA

Facultad de Ingeniería

Maestría en Hidrología con mención en Ecohidrología

Improving reference evapotranspiration (ET_0) calculation under limited data conditions in the high Tropical Andes

Trabajo de titulación previo a la obtención del título de Magíster en Hidrología con mención en Ecohidrología

Autora:

Cristina Alejandra Vásquez Ojeda

CI:1105025223

Correo electrónico: criz5.aleja@gmail.com

Director:

Galo José Carrillo Rojas, PhD.

CI: 0101799096

Cuenca, Ecuador

04-marzo-2021



Resumen

El cálculo de la evapotranspiración del cultivo de referencia (ET_o) utilizando la ecuación FAO56 Penman-Monteith ($PM-ET_o$) requiere datos sobre las temperaturas máxima y mínima del aire (T_{max} , T_{min}), la humedad relativa (RH), la radiación solar (R_s) y el viento. velocidad (u_2). Sin embargo, los registros de las variables meteorológicas suelen ser incompletos o de mala calidad. Con frecuencia, en las zonas montañosas como las de los Andes, los sensores ambientales están sujetos a duras condiciones, debido a la variabilidad climática diurna / nocturna que genera condiciones desafiantes para el monitoreo meteorológico, lo que conduce a la pérdida de datos. Para paisajes de gran altitud como los Andes, las variables faltantes de déficit de presión de vapor y radiación solar causan un alto impacto en el cálculo de $PM-ET_o$. Para evaluar estas limitaciones, en la presente investigación se han considerado varios métodos que se basan en la temperatura máxima y mínima para estimar las variables faltantes. Con base en datos de tres estaciones meteorológicas automáticas en los Andes tropicales altos (páramo húmedo, 3298 - 3955 m s.n.m.), encontramos que la calibración y validación de métodos fueron esenciales para estimar R_s . Utilizando el método de De Jong y Stewart (1993) (R_s-DS) obtuvimos el rendimiento más alto, un RMSE entre 2,89 y 3,81 MJ m⁻² día⁻¹. Además, en ausencia de observaciones de HR, reemplazar la temperatura del punto de rocío (T_{dew}) por T_{min} fue una alternativa confiable, cuando se aplicó el método de Allen et al. (1998) (VPD-FAO) que mostró el mayor desempeño con RMSE entre 0.08 y 0.12 kPa. Estos resultados arrojaron estimaciones de $PM-ET_o$ altamente precisas, con RMSE entre 0,29 y 0,34 mm día⁻¹ y RMSE entre 0,12 y 0,18 mm día⁻¹, respectivamente. Como era de esperar, cuando faltaban ambas variables, el cálculo de ET_o aumentó su error, con un RMSE entre 0,32 y 0,42 mm día⁻¹. Una estimación adecuada de ET_o en el páramo andino contribuye a mejorar la productividad del agua para usos domésticos e industriales, agricultura de regadío e hidroeléctrica.

Palabras claves: Páramo. $PM-ET_o$. Radiación solar. Déficit de presión de vapor. Calibración.

**Abstract**

The computation of the reference crop evapotranspiration (ET_o) using the FAO56 Penman-Monteith equation (PM- ET_o) requires data on maximum and minimum air temperatures (T_{max} , T_{min}), relative humidity (RH), solar radiation (R_s), and wind speed (u_2). Nevertheless, the records of meteorological variables are often incomplete or of poor quality. Frequently, in the mountain areas such as those of the Andes, environmental sensors are subject to harsh conditions, due to the diurnal/nocturnal climatic variability causing challenging conditions for meteorological monitoring, which leads to data loss. For high-elevation landscapes like the Andes, the missing variables of vapor pressure deficit and solar radiation cause a high impact on PM- ET_o calculation. To assess these limitations, several methods relying on maximum and minimum temperature to estimate the missing variables have been considered in the present investigation. Based on data from three automatic weather stations in the high Tropical Andes (humid páramo, 3298 – 3955 m a.s.l.), we found that the calibration and validation of methods were essential to estimate R_s . Using the De Jong and Stewart (1993) (R_s -DS) method we retrieved the highest performance, a RMSE between 2.89 and 3.81 MJ $m^{-2} day^{-1}$. Moreover, In the absence of RH observations, replacing the dew point temperature (T_{dew}) by T_{min} was a reliable alternative, when apply the method of Allen et al. (1998) (VPD-FAO) which showed the highest performance with RMSE between 0.08 and 0.12 kPa. These results yielded highly accurate PM- ET_o estimates, with RMSE between 0.29 and 0.34 mm day^{-1} and RMSE between 0.12 and 0.18 mm day^{-1} , respectively. As expected, when both variables were missing, the ET_o calculation increased its error, with an RMSE between 0.32 and 0.42 mm day^{-1} . A proper estimation of ET_o in the Andean páramo contributes to improved water productivity for domestic and industrial uses, irrigated agriculture, and hydropower.

Keywords: Páramo. PM- ET_o . Solar radiation. Vapor pressure deficit. Calibration.



INDEX

Resumen 2

Abstract 3

INDEX OF FIGURES 4

Cláusula de licencia y autorización para publicación en el Repositorio Institucional..... 5

Cláusula de Propiedad Intelectual..... 6

1 Introduction 7

2 Study Area and Data..... 9

3 Methods..... 11

 3.1 Estimation of Solar Radiation..... 12

 3.1.1 Methods to estimate R_s 12

 3.1.2 Data Preprocessing 14

 3.1.3 Calibration and Validation of R_s estimation methods..... 15

 3.2 Methods to estimate VPD 16

 3.3 Impact of R_s and VPD estimation on PM- ET_o calculation 18

 3.4 Evaluation criteria 19

4 Results and discussion 19

 4.1 Estimation of Solar Radiation (period 2014-2017)..... 19

 4.2 Estimation of Vapor Pressure Deficit (period 2014-2017)..... 21

 4.3 Estimation of daily ET_o when R_s and/or VPD are missing (period 2018-2019)
 22

5 Conclusions 31

6 References 32

INDEX OF FIGURES

Fig. 1. Study area and the location of weather stations in the Quinoas Ecohydrological Observatory. 10

Fig. 2. Flowchart of the PM- ET_o calculation with estimation of R_s and VPD. 12

Fig. 3. Duration curve of the difference between the maximum and minimum daily air temperature by weather station..... 15

Fig. 4. Comparison of daily R_s observed and estimated (with five methods) in all stations (Chirimachay, Virgen and Toreadora). The solid line represents the fitted regression line. The dashed line indicates 1:1..... 27

Fig. 5. Comparison of daily observed and estimated VPD (with four methods) in all stations (Chirimachay, Virgen and Toreadora). The solid line represents the fitted regression line. The dashed line indicates 1:1..... 28

Fig. 6. Comparison of daily PM- ET_o and PM- ET_o R_s -DS and/or VPD-FAO in all stations: Chirimachay, Virgen and Toreadora. The solid line represents the fitted regression line. The dashed line indicates 1:1. 30



Cláusula de licencia y autorización para publicación en el Repositorio Institucional

Cristina Alejandra Vásquez Ojeda en calidad de autora y titular de los derechos morales y patrimoniales del trabajo de titulación "**Improving reference evapotranspiration (ET_o) calculation under limited data conditions in the high Tropical Andes**", de conformidad con el Art. 114 del CÓDIGO ORGÁNICO DE LA ECONOMÍA SOCIAL DE LOS CONOCIMIENTOS, CREATIVIDAD E INNOVACIÓN reconozco a favor de la Universidad de Cuenca una licencia gratuita, intransferible y no exclusiva para el uso no comercial de la obra, con fines estrictamente académicos.

Asimismo, autorizo a la Universidad de Cuenca para que realice la publicación de este trabajo de titulación en el repositorio institucional, de conformidad a lo dispuesto en el Art. 144 de la Ley Orgánica de Educación Superior.

Cuenca, 04 de marzo de 2021

Cristina Alejandra Vásquez Ojeda

C.I: 1105025223



Cláusula de Propiedad Intelectual

Cristina Alejandra Vásquez Ojeda, autora del trabajo de titulación "**Improving reference evapotranspiration (ET_o) calculation under limited data conditions in the high Tropical Andes**", certifico que todas las ideas, opiniones y contenidos expuestos en la presente investigación son de exclusiva responsabilidad de su autora.

Cuenca, 04 de marzo de 2021

Cristina Alejandra Vásquez Ojeda

C.I: 1105025223



1 Introduction

The páramo is the most important ecosystem in the high Tropical Andes for water resources supply (Hofstede et al., 2014). The Andean páramo covers over 30,000 km² of northern South America (Wright et al., 2018). It is the primary water source for communities located near this ecosystem, which include major cities in Colombia, Ecuador, and Perú (Buytaert et al., 2006). Its vegetation consists mainly of tussock grasses, cushion plants, and patches of woody species such as *Polylepis* sp. and *Gynoxys* sp. that occur only in sheltered locations and along water streams (Buytaert et al., 2006). This ecosystem serves as a sponge that captures precipitation, stores, and releases the water gradually to the surrounding areas (Llambí, et al. 2012) producing a sustained streamflow during the year. This water resource is intensively used for irrigated agriculture, industry, rural, and urban drinking water systems, hydro-power production, and for sustaining aquatic ecosystems (Céleri and Feyen, 2009; Llambí et al., 2012). Particularly an important economic function of water in Andean ecosystems is to irrigate agriculture in downstream areas. At present, irrigation represents 71.2%, which becomes the activity that consumes the most flow in our country. Compromising almost all of the water sources located in high altitude areas for irrigation (Ministerio de Agricultura y Ganadería et al., 2019).

Although evapotranspiration may not be a limiting factor for water use in cold and humid regions, the increasing demand for water resources due to population growth, urbanization, and irrigated agriculture require a reliable estimate of evapotranspiration to improve the yield and water productivity. A common approach for calculating evapotranspiration is the estimation of ET_o , which is the most useful for countless scientific and management applications, such as water balance studies at different scales, evaluation of water resources, and development of watershed management plans. Likewise, ET_o plays a key role in crop water, irrigation planning and management, as well as in studies related to the analysis of climate change and water conservation (Paredes et al., 2020, 2017; Todorovic et al., 2013).

According to the Food and Agriculture Organization (FAO56) (Allen et al., 1998), the Penman-Monteith equation (PM) is the most recommended method to determine ET_o . This method is a global standard based on meteorological data (Allen et al., 1998) and their applications all over the world have been quite successful (Jabloun and Sahli, 2008; Ochoa-Sánchez et al., 2019; Paredes et al., 2020, 2017; Paredes and Pereira, 2019; Todorovic et al., 2013). Nevertheless, the major limitation of the Penman-Monteith



equation reported in many studies is the requirement of meteorological variables (air temperature, relative humidity, solar radiation, and wind speed) that are often incomplete or of poor quality (Córdova et al., 2015; da Silva et al., 2018; Karimi et al., 2020; Paredes and Pereira, 2019; Santos et al., 2020; Sentelhas et al., 2010; Tomas-Burguera et al., 2017). This usually happens when a sensor breaks or malfunctions (e.g., due to weather conditions, lack of maintenance, or electronic failure). Frequently, in the mountain areas, like the Andes, sensors are subject to harsh environmental conditions, due to the high climatic variability during the day causing challenging environmental conditions for meteorological monitoring, which leads to data loss. Accordingly, the application of PM faces the problem of data unavailability.

Research has developed a variety of tools and procedures to overcome the unavailability of data by using empirical equations, most of them relying on maximum and minimum temperature. For instance, the procedures by George H. Hargreaves and Zohrab A. Samani (1982), the equations proposed in FAO56 (Allen et al., 1998), the equations by Castellví et al. (1997), among others. However, these methods require local calibrations to obtain satisfactory performances as several studies have shown in various climate types ranging from hyper arid to humid (Karimi et al., 2020; Paredes et al., 2017; Raziei and Pereira, 2013; Ren et al., 2016; Todorovic et al., 2013). The approach of these studies was the calibration of the K_{RS} coefficient of the George H. Hargreaves and Zohrab A. Samani (1982) method to estimate solar radiation when the variable was missing, and a correction in the minimum temperature to estimate actual vapor pressure in the absence of relative humidity data. In all cases, their results showed that the PM- ET_o method had greater precision in both arid and humid climates when missing data was estimated. Nevertheless, Todorovic et al. (2013) found that for good ET_o performance, the correction applied in the minimum temperature was only necessary for hyper-arid, arid, semi-arid, and dry subhumid climates and not for humid conditions. Moreover, Ren et al. (2016) found that the calibrated coefficient of the method to estimate solar radiation varied with climatic aridity. The errors of estimates were higher when the range of variation of ET_o was higher, which occurred more often for hyper-arid and arid climates contrarily to sub-humid locations. In addition, Karimi et al. (2020) also found that the effect of using estimated values of solar radiation on PM- ET_o calculation caused greater error than using estimated values of wind speed.

Unlike the most common methods reviewed above, in various studies, a large number of empirical methods are compared to estimate the missing variables (Bandyopadhyay et al., 2008; Besharat et al., 2013; Jabloun and Sahli, 2008; Li et al., 2013; Tabari et al., 2016). Nonetheless, there is a shortage of information for high-elevation landscapes like



the Andes, contrary to the information available in low and arid areas. Using daily data recorded from eight weather stations in North Africa (Tunisia), Jabloun and Sahli (2008) evaluated the performance of the PM-ET_o method with limited data and revealed that estimating solar radiation with Allen. R (1995) method that takes into account the elevation effects on the volumetric heat capacity of the atmosphere, it gave accurate estimates of ET_o in all the studied regions. Furthermore, the use of minimum temperature was a good alternative when relative humidity measurements were lacking. The use of the mean annual wind speed of the location led to acceptable ET_o estimates, especially for high ET_o rates. Under cool, arid, and semi-arid conditions in Iran, Tabari et al. (2016) estimated solar radiation using 12 models and then compared daily PM-ET_o values derived from both measured and estimated solar radiation. The results indicated that using estimated R_s, the PM-ET_o method performed well for semi-arid and arid climates. In cold conditions, the PM-ET_o accuracy decreased despite the calibration of the models.

To the best of our knowledge, there is only one previous study that examined the impact of missing meteorological variables on PM-ET_o calculation in the high Tropical Andes. Córdova et al. (2015) evaluated the PM-ET_o equation with limited data using meteorological variables of two weather stations in the high Tropical Andes (Ecuador) and found that the maximum error in ET_o calculations was observed when solar radiation and relative humidity were missing, while wind speed had a much lower impact. Finally, they concluded that there is an urgent need for the development of alternative methods in these sites to estimate accurate values for missing variables. Nevertheless, there is a knowledge gap to estimate the missing variables and this makes PM-ET_o subject to high uncertainty. Thus, the first step to achieving this is to develop or calibrate equations to estimate the missing variables and then evaluate its impact on PM-ET_o.

Therefore, the objectives of this study are (a) To calibrate and validate methods to estimate R_s, (b) To evaluate the performance of methods to estimate Vapor Pressure Deficit (VPD) and, (c) To evaluate the impact on PM-ET_o calculation when R_s and/or VPD are missing for the paramo ecosystem.

2 Study Area and Data

In the Tropical Andes of southern Ecuador, the headwater catchment of Quinoas covers an area of about 94.1 km² and an elevation range of 3150 to 4425 m a.s.l. (Fig. 1). The Quinoas catchment is characterized as a Páramo ecosystem. This bioma stores large amounts of water that is captured from rainfall events, drizzle, and fog interception (Beck

et al., 2008). The climate is influenced by air masses of both the Pacific and the Amazon basin (Buytaert et al., 2006). A bimodal precipitation seasonality is presented, in connection with the meridional displacement of the Intertropical Convergence Zone (ITCZ) and its double passage throughout the year over the deep tropics (Garreaud, 2009). This corresponds to the months from March to May and October where the maximum values of precipitation are recorded (Carrillo-Rojas et al., 2016). Annual precipitation is between 946 and 1120 mm. The Table 1 describes the daily values of different meteorological variables. These values coincide with those reported by Córdova et al. (2015) and Carrillo-Rojas et al. (2016) in the same study site.

Meteorological data were collected along an altitudinal gradient (3298 - 3955 m a.s.l.) during the six-year period 2014-2019 from three automatic weather stations (AWSs): Chirimachay, Virgen del Cajas (hereafter denoted as Virgen) and Toreadora. All measurements were made at 2m above ground level. Each station recorded data at a 5-minute frequency for average temperature (T_{avg}), T_{max} , T_{min} , average relative humidity (RH_{avg}), maximum relative humidity (HR_{max}), minimum relative humidity (HR_{min}), u_2 and R_s . The values were aggregated on a daily scale. Due to the presence of gaps in the database, preprocessing was performed, excluding days with missing data. The amount of missing data was 3.7%, 2.5%, and 6.8% for Chirimachay, Virgen, and Toreadora AWSs, respectively. The sensors used in the study are described in Table A1, Appendix A.

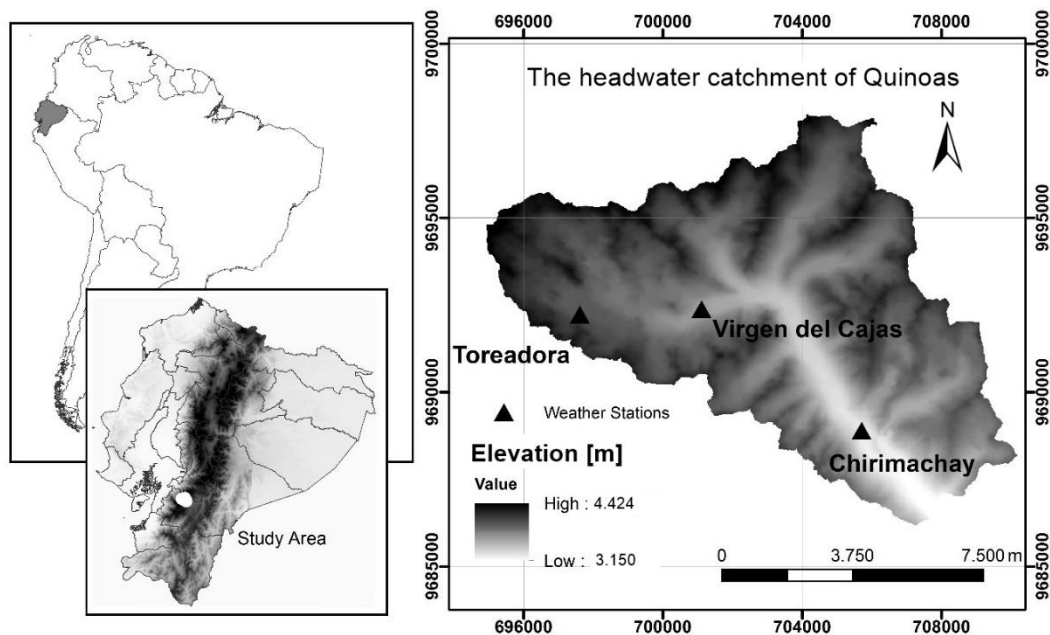


Fig. 1. Study area and the location of weather stations in the Quinoas Ecohydrological Observatory.

**Table 1**

Summary of daily meteorological variables during the study period 2014 – 2019.

Station name	Latitude and Longitude (UTM)	Elev. (m a.s.l.)	T _{avg} (°C)	T _{max} (°C)	T _{min} (°C)	RH _{avg} (%)	RH _{max} (%)	RH _{min} (%)	R _s (MJ m ⁻² day ⁻¹)	U _{2m} (m s ⁻¹)	ET _o (m m day ⁻¹)
Chirimachay	9688896;-705704	3298	8.73	19.48	-1.35	85.26	100	8.81	10.12	1.38	1.88
Virgen	9623820;-701111	3626	6.68	17.94	-3.92	83.01	100	9.52	11.56	1.58	1.98
Toreadora	9692227;-697619	3955	5.46	17.15	-2.44	83.98	100	6.30	11.88	2.18	1.92

3 Methods

We followed the flowchart presented in Fig. 2. First, to estimate R_s (section 3.1), we selected five different methods based on air temperature. These methods have coefficients that were calibrated and validated in order to obtain satisfactory performances. Prior to calibration, we performed a data preprocessing to capture all the temperature variability in the calibration and validation datasets. Then, we evaluated the ability of each method to simulate R_s in order to select the method with the best performance. Second, to estimate the VPD (section 3.2.), we selected four different methods also based on air temperature. Then, we evaluated the ability of each method to estimate VPD in order to select the method with the best performance. Finally, with the methods selected previously, we evaluated the impact of R_s and VPD estimation on PM-ET_o calculation (section 3.3). The methodological details are explained in the following subsections.

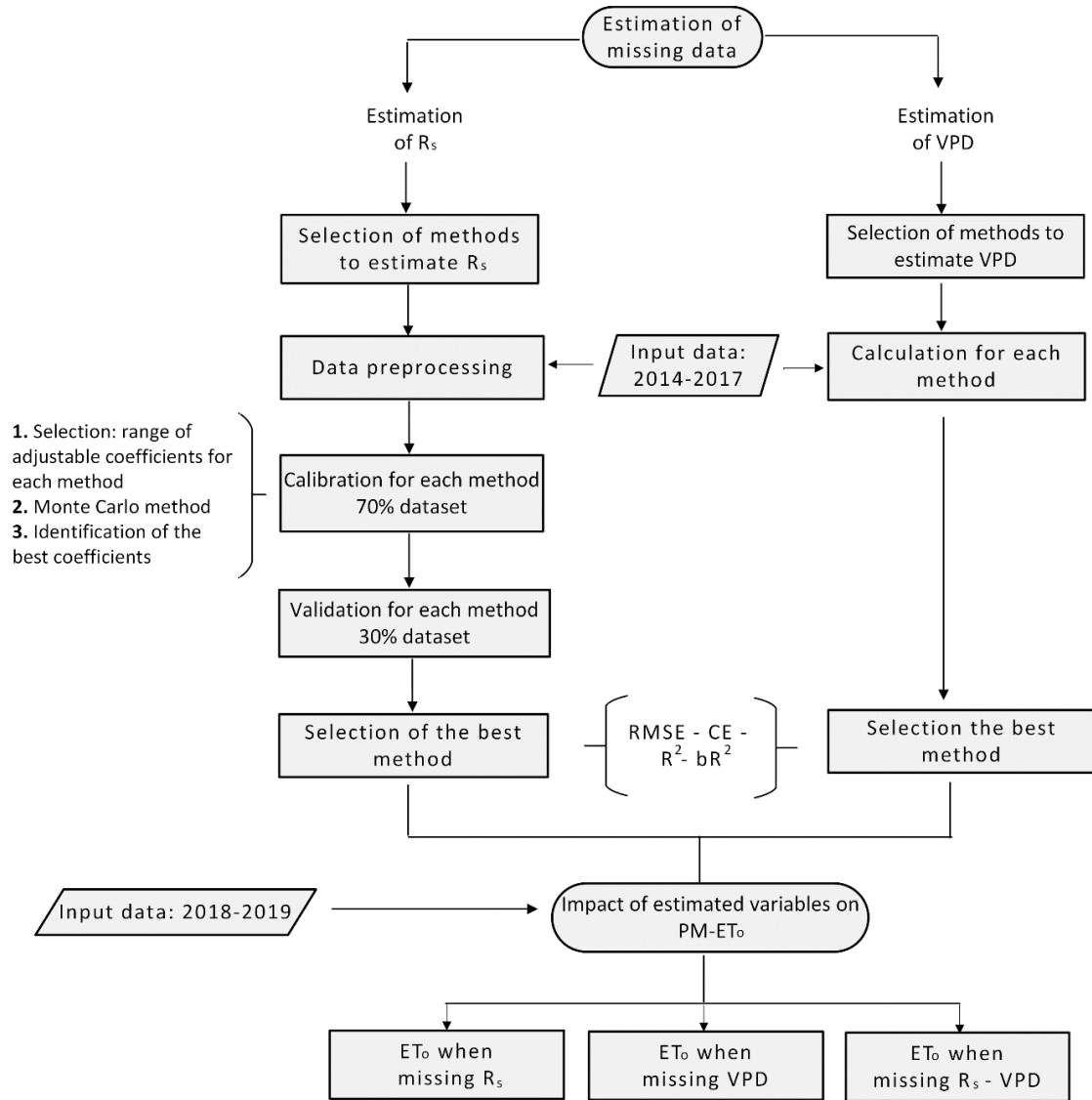


Fig. 2. Flowchart of the PM-ET₀ calculation with estimation of R_s and VPD.

3.1 Estimation of Solar Radiation

3.1.1 Methods to estimate R_s

George H. Hargreaves and Zohrab A. Samani (1982) – hereafter denoted as R_s-HS – recommended a method to estimate solar radiation using the difference between the maximum and minimum temperature. This is related to the degree of cloud cover in a given location:

$$R_s = K_{RS} \sqrt{T_{max} - T_{min}} R_a \quad (1)$$



where K_{RS} is an adjustment coefficient. The authors recommended K_{RS} values from 0.16 to 0.19, (0.16 for inland regions and 0.19 for coastal regions). R_a is extraterrestrial radiation ($\text{MJ m}^{-2} \text{ day}^{-1}$) (Allen et al., 1998):

$$R_a = 37.6dr (t \cdot \sin\varphi \cdot \sin\delta + \cos\varphi \cdot \cos\delta \cdot \sin t) \quad (2)$$

where dr is the reverse relative distance Earth-Sun (Eq. 3), t is the radiation angle at sunset (Eq. 4), δ is the solar declination (rad) (Eq. 5) and φ is the latitude of the location. J is the Julian day of the year (from 1 to 365 and from 1 to 366 for leap years):

$$dr = 1 + 0.033 \cos(2\pi/365) J \quad (3)$$

$$t = \arccos(-\tan\varphi \cdot \tan\delta) \quad (4)$$

$$\delta = 0.4093 \sin((2\pi/365) J - 1.39) \quad (5)$$

De Jong and Stewart (1993) – hereafter denoted as R_s -DS – suggested using the following equation incorporating precipitation and the range of daily temperature (ΔT):

$$R_s = a * R_a * (\Delta T)^b * (1 + cp + dp^2) \quad (6)$$

where a , b , c and d are adjustment coefficients, p is precipitation in mm, and ΔT can be calculated as:

$$\Delta T = (T_{max}) - \frac{T_{min(j)} + T_{min(j+1)}}{2} \quad (7)$$

where T_{max} is the daily maximum temperature ($^{\circ}\text{C}$), $T_{min(j)}$ and $T_{min(j+1)}$ are the daily minimum temperature ($^{\circ}\text{C}$) of the corresponding and the next day, respectively.

Allen, R (1995) – hereafter denoted as R_s -AL – modified equation 1 by estimating K_{RS} as a function of the ratio of atmospheric pressure:

$$k_{RS} = k_{RA} \left(\frac{P}{P_0}\right)^{0.5} \quad (8)$$



where k_{RA} is an adjustment coefficient having values in the 0.17-0.20 range, with values of 0.17 for inland regions and 0.20 for coastal regions; and P is the mean atmospheric pressure of the site (kPa); P_0 is the mean atmospheric pressure at sea level (101.3 kPa):

$$P = P_0 \left(\frac{293 - 0.0065Z}{293} \right)^{5.26} \quad (9)$$

where Z is the elevation (m a.s.l.) of the site.

Vanderlinden et al. (2004) – hereafter denoted as R_s -VA – found a relationship between the adjustment coefficient, k_{RS} , and the mean, minimum and maximum daily air temperatures:

$$k_{RS} = a * \left(\frac{T_{mean}}{TD} \right) + b \quad (10)$$

where a and b are adjustment coefficients, $T_{mean} = (T_{max} + T_{min})/2$ and $TD = T_{max} - T_{min}$.

Chen et al. (2004) – hereafter denoted as R_s -CH – found a logarithmic relationship between daily solar radiation, daily extra-terrestrial solar radiation, and the difference between the maximum and minimum daily air temperature:

$$R_s = a \ln (T_{max} - T_{min}) - b * R_a \quad (11)$$

where a and b are adjustment coefficients.

3.1.2 Data Preprocessing

To avoid a bias in the selection of the samples for calibration and validation, we performed a data preprocessing. A duration curve was made for $T_{max} - T_{min}$ (this variable serves as input for the aforementioned methods) for each weather station (Fig. 3). This analysis was made because, in preliminary calculations, random samples containing a disproportionately large percentage of high or low values caused a biased calibration of the methods (not shown). The curves showed inflection points around the 20th and the 90th percentiles in the three stations (limits indicated by the solid vertical lines in Fig. 3), which were set as the limits for the different groups of data. Therefore, the data was split



into three sets: high values ($\leq 20\%$), medium values ($>20\%$ and $\leq 90\%$) and low values ($>90\%$) (Fig. 3). This data classification was subsequently used for assembling the groups for the calibration and validation processes (Section 3.1.3).

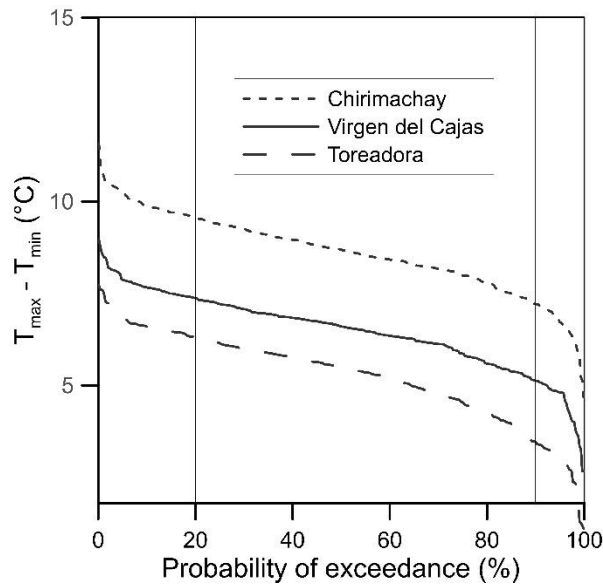


Fig. 3. Duration curve of the difference between the maximum and minimum daily air temperature by weather station.

3.1.3 Calibration and Validation of R_s estimation methods

A model performs better when calibration is performed with a large dataset enough to contain a wide range of weather conditions (Motavita et al., 2019; Perrin et al., 2007; Xia et al., 2004). Motavita et al. (2019) also mentioned that in the calibration and validation datasets must contain a wide range of the variability. Bennett et al. (2013) suggested randomizing the division of data, so that the model performance is not biased by the allocation of data. Following these recommendations, we took the first 4 years of data for calibration and validation (2014-2017), and took 70% of the data for calibration, while 30% was left for validation. The calibration and validation samples were taken randomly but considering that each subset must fit the distribution criteria described in section 3.1.2: 20% of high values, 70% of medium values, and 10% of low values.

In order to find a general method for the ecosystem, calibration was performed for the entire altitudinal gradient, by analyzing all data from the three weather stations combined as the methodology of De Jong and Stewart (1993) applied in their study. The Monte Carlo method was used to select the optimal coefficients after performing 5,000 simulations. The ranges of the adjustable coefficients for each method were selected



according to previous studies (Table A2, Appendix A). For each method, we selected the coefficients with the highest Nash–Sutcliffe efficiency (CE). However, other performance indexes such as Root Mean Square Error (RMSE), Coefficient of Determination (R^2), and Coefficient of Determination multiplied by the slope (bR^2) were additionally calculated to provide more information about the quality of the simulation. Moreover, we validated each calibrated method with data independent of the calibration. After running the calibration and validation for the altitudinal gradient, we applied the calibrated methods with the data of each station.

3.2 Methods to estimate VPD

Vapor Pressure Deficit is estimated as the difference between the saturation vapor pressure, e_s , and the actual vapor pressure, e_a :

$$VPD = e_s - e_a \quad (12)$$

where e_s is calculated as:

$$e_s = \frac{e^\circ(T_{max}) + e^\circ(T_{min})}{2} \quad (13)$$

and when relative humidity data is available, e_a is calculated as:

$$e_a = \frac{e^\circ(T_{min}) \frac{RH_{max}}{100} + e^\circ(T_{min}) \frac{RH_{min}}{100}}{2} \quad (14)$$

where $e^\circ(T)$ is the saturation vapor pressure (kPa), and T_{max} and T_{min} are the maximum and minimum daily temperature ($^\circ\text{C}$) and RH_{max} and RH_{min} are the maximum and minimum daily relative humidity. $e^\circ(T)$ for air temperature T is:



$$e^{\circ}(T) = 0.6108 \exp \exp \left[\frac{17.27 * T}{T * 237.3} \right] \quad (15)$$

In the absence of humidity data, we evaluated four different methods based on air temperature to estimate the daily VPD, using four years of data (2014-2017).

In FAO56 Allen et al. (1998) – hereafter denoted as VPD-FAO – stated that e_a may be obtained by assuming that the dewpoint temperature, T_{dew} , is close to the T_{min} , which is usually experienced at sunrise in reference weather stations. However, because of the high humidity in our study area causes the RH reaching 100% most of the nighttime hours, we used the minimum daily temperature between 05H00 and 08H00 for T_{dew} . e_a is calculated by:

$$e_a = e^{\circ}(T_{dew}) = 0.6108 \exp \exp \left[\frac{17.27 * T_{dew}}{T_{dew} * 237.3} \right] \quad (16)$$

Doorenbos and Pruitt (1977) – hereafter denoted as VPD-DP – proposed the following method to estimate VPD:

$$VPD = e^{\circ}(T_{avg}) - e^{\circ}(T_{dew}) \quad (17)$$

where $e^{\circ}(T_{avg})$ is the saturation vapor pressure at the mean daily temperature.

Castellví et al. (1997) – hereafter denoted as VPD-CA1 – proposed the following method to estimate VPD:

$$VPD = e^{\circ}(T_a) - e^{\circ}(T_{dew}) \quad (18)$$

where T_a defined as the temperature that leaves equal areas under the curve $e^{\circ}(T) - e^{\circ}(T_{dew})$ between T_{max} and T_{min} using the trapezoidal method, for more detail review the research of Castellví et al. (1997).



Castellví et al. (1997) – hereafter denoted as VPD-CA2 – proposed the following method to estimate the mean relative humidity:

$$RH_{avg} = 100 * \frac{e^{\circ}(T_{dew})}{\frac{1}{2}[e^{\circ}(T_a) + e^{\circ}(T_{avg})]} \quad (19)$$

then, we calculated e_a as proposed FAO56 (Allen et al., 1998):

$$e_a = \frac{RH_{avg}}{100} e^{\circ}(T_{avg}) \quad (20)$$

3.3 Impact of R_s and VPD estimation on PM-ET_o calculation

We used two years of complete data (2018-2019) to calculate PM-ET_o, then we generated missing data scenarios by removing R_s or/and VPD values, and evaluated the impact on PM-ET_o calculation when these variables were estimated using the selected equations previously.

The PM-ET_o method defined by Allen et al. (1998) for calculating reference evapotranspiration of a hypothetical crop having a height of 0.12 m, a surface resistance of 70 s m⁻¹ and an albedo of 0.23 is:

$$PM - ET_O = \frac{0.408\Delta(R_n - G) + \gamma(900 / (T_{avg} + 273))u_2(e_s - e_a)}{\Delta + \gamma(1 + 0.34u_2)} \quad (21)$$

where R_n is the net radiation at the crop surface (MJ m⁻² day⁻¹), G is the soil heat flux density (MJ m⁻² day⁻¹), T_{avg} at 2 m (°C), u_2 is the wind speed at 2 m (m s⁻¹), e_s is the saturation vapor pressure (kPa), e_a is the real vapor pressure (kPa), $e_s - e_a$ is the vapor pressure deficit (kPa), Δ is the slope of the vapor pressure curve (kPa °C⁻¹) and γ is the psychrometric constant (kPa °C⁻¹). For daily computations, G equals zero as the magnitude of daily soil heat flux beneath the grass reference surface is very small (Allen et al., 1998).



3.4 Evaluation criteria

The statistical indices used to evaluate the methods performance were: i) the Nash–Sutcliffe efficiency (CE), which has been widely used to evaluate the performance of empirical models and it is sensitive to differences in the observed and simulated means and variances; ii) the coefficient of determination (R^2), which describes how much of the observed dispersion is explained by the prediction; iii) the coefficient of determination multiplied by the slope (br^2), and, iv) the root mean square error ($RMSE$), which is a weighted measure of the error in which the largest deviations between the observed and modeled values contribute the most (Table A3, Appendix A). To evaluate the quality of the PM-ET_o calculations when one or two variables were missing, we used the same statistical indices.

4 Results and discussion

4.1 Estimation of Solar Radiation (period 2014-2017)

As previously stated, in the absence of R_s observations, this variable was estimated using methods based on air temperature with locally calibrated adjustment coefficients (Eq. 1-11). Table 2 shows the coefficients and statistical indicators of the calibration of the methods to estimate R_s .

When we combined the data from the three stations to calibrate the methods and to select the best method for the gradient, it was found that the adjustment coefficients of each method varied from their original values. In a global context, the difference of the coefficients is related to the different climatic regions where the methods have been developed and tested. These methods have been mostly applied in arid and semi-arid regions, and to a lesser degree in humid regions. In the available literature it was found that to estimate R_s , the authors commonly use the recommendations of Allen, R (1995) and George H. Hargreaves and Zohrab A. Samani (1982) with a local calibration of the k_{RS} coefficient (Jabloun and Sahli, 2008; Paredes et al., 2020, 2017; Paredes and Pereira, 2019). In such studies, the k_{RS} coefficient ranged from 0.14 to 0.22 for the R_s -HS method and for the R_s -AL method the literature showed values from 0.15 to 0.18. While in our study area, k_{RS} had lower values in both cases. The variability of the coefficients is influenced by the change in the range of the maximum and minimum temperature difference (DTR), where the K_{RS} values become lower when the DTR range



decreases. The R_s -CH method showed values in the range of 0.16 to 0.42 (coefficient a) and -0.45 to 0.12 (coefficient b) in the North China Plain (Chen et al., 2004). In our case, the calibration had lower values. However, the behavior was similar to that found by Li et al. (2014) and Liu et al. (2009), who reported that at higher altitudes, the coefficient a increases and the coefficient b decreases. The R_s -VA method showed average values of 0.0030 and 0.0022 for the coefficients a and b , respectively, in Southern Spain (Vanderlinden et al., 2004), while we found higher values in our study. On the other hand, for the R_s -DS method, the values of the coefficients a (0.127), b (0.599), c (-0.028) and d (0.0003) reported in western Canada (De Jong and Stewart, 1993) were similar to our values, except by the coefficient a that was greater. For a detailed comparison of coefficients, see Table 2.

The methods that use DTR as input (R_s -HS, R_s -AL, R_s -VA, and R_s -CH) had similar performance, showing a RMSE in the range from 3.58 to 3.73 MJ m⁻² day⁻¹, a CE from 0.42 to 0.47, and R^2 and bR^2 values from 0.47 to 51 and from 0.43 to 0.47, respectively. Whereas the R_s -DS method that used ΔT and the effect of precipitation (Eq. 6-7), yielded better estimations than the other methods with higher values of CE, R^2 , and bR^2 , and a lower value of RMSE (Table 2).

Table 3 presents the results of the validation for the methods in the altitudinal gradient. It was observed that the performance of the R_s -HS, R_s -AL, R_s -VA and R_s -CH methods was similar to the calibration performance, and it was confirmed that R_s -DS method is the highest performing one.

Once the methods were calibrated for the gradient, we evaluated them using the data from each station individually. The scatter plot for Chirimachay (Fig. 4a,d,g,j,m) showed high dispersion and slight overestimation for R_s below 15 MJ m⁻² day⁻¹. This was reflected in a slight increase in RMSE and a lower CE compared to the results obtained for the entire gradient. Moreover, the R_s -DS and R_s -AL methods showed the best results, a lower RMSE and a higher CE, R^2 and bR^2 . However, these results did not differ greatly from the performance of the rest of the methods at the site (Table 4).

We found that Virgen had the best adjustment to the observed values in all the methods in comparison to the other sites, and the method with the best performance was R_s -DS (Table 4; Fig. 4b,e,h,k,n). In Toreadora, the CE presented the lowest values compared to the other sites for all the methods except for R_s -DS. This method showed the best performance to estimate R_s at the site (Table 4).



In addition, we found that the ability of the methods to estimate R_s is affected by elevation, because there is a major incidence of solar radiation in high areas; nonetheless, such effect on the temperature is low. This is due to the fact that only a small fraction of R_s is absorbed by the thinner atmosphere of these high elevation sites (Llambí et al., 2012). This means that the incoming R_s does not heat up, and this is reflected in the underestimation of high values of R_s . Therefore, at the highest site, Toredora, the highest values of R_s resulted in the lowest accuracy ($bR^2 < 0.51$) in all methods compared to the other sites. At this location, the methods that used DTR (R_s -HS, R_s -AL, R_s -VA and R_s -CH) estimated R_s values up to $15 \text{ MJ m}^{-2} \text{ day}^{-1}$ (80 % of data) and the R_s -DS method (which uses ΔT and the effect of precipitation) estimated R_s values up to $19 \text{ MJ m}^{-2} \text{ day}^{-1}$ (90 % of data). While for the Chirimachay and Virgen sites, the R_s -HS, R_s -AL, R_s -VA and R_s -CH methods presented difficulty in estimating $R_s > 17 \text{ MJ m}^{-2} \text{ day}^{-1}$ (12.86 % of data), and the R_s -DS method estimated R_s values up to $21 \text{ MJ m}^{-2} \text{ day}^{-1}$ (93.24 % of data) (Fig. 4).

According to Samani (2000), the performance of the methods based on temperature increases as DTR increases. Therefore, this performance decreases with the altitude, because DTR is reduced. Evidently, our results agree with this elevation effect that causes DTR to decrease in the highest site. This finding is also consistent with the results presented by Paredes et al. (2017). They showed an underestimation of the high values of R_s in the sites with higher elevation and thus lower DTR. As well as Li et al. (2014) in China and Bandyopadhyay et al. (2008) in India, who reported the failure of these methods for high elevation stations.

4.2 Estimation of Vapor Pressure Deficit (period 2014-2017)

Table 5 summarizes the statistical indicators of the methods applied to estimate daily VPD. It was found that in the gradient the RMSE was in the range from 0.08 to 0.30 kPa, the CE with values between 0.24 to 0.63, the R^2 with values between 0.55 a 0.81, and bR^2 from 0.35 to 0.71. The VPD-FAO method had the highest performance in most of the statistical indicators, but also showed a slight overestimation for low and medium values. In addition, an underestimation of low values was found using the VPD-DP, VPD-CA1 and VPD-CA2 methods in Chirimachay and an overestimation of medium values by the VPD-CA1 and VPD-CA2 methods in Virgen and Toredora (Fig. 5).

To find the best method for the gradient, we analyzed the statistics site by site. In Chirimachay, the VPD-FAO method had the best performance with the highest R^2 and



bR^2 and a low RMSE (0.12 kPa). In Virgen and Toredora the VPD-FAO method had the lowest RMSE with values of 0.08 and 0.09 kPa, respectively. The other statistical results confirmed that the VPD-FAO method had the highest performance (Table 5).

Therefore, we conclude that the VPD-FAO method is the most suitable method to estimate VPD in the altitudinal gradient. However, the overestimation presented by this approach has also been found in other studies performed in humid climates (Landeras et al., 2008; Paredes et al., 2017; Todorovic et al., 2013; Tomas-Burguera et al., 2017). This could be due to the fact that $T_{\text{dew}} > T_{\text{min}}$ in sub-humid and humid climates (Paredes et al., 2017; Todorovic et al., 2013). Hence, by assuming $T_{\text{dew}} = T_{\text{min}}$, e_a is being underestimated and therefore VPD is overestimated. In fact, a previous analysis showed that when we took the daily minimum temperature the overestimation was 0.04 kPa per day greater than the current one. To decrease this overestimation, we took the minimum temperature at sunrise (05H00 – 08H00) to get closer to the actual value of T_{dew} .

4.3 Estimation of daily ET_o when R_s and/or VPD are missing (period 2018-2019)

Table 6 shows the statistical performance of the PM- ET_o calculation when R_s and/or VPD were missing and were estimated with the best methods selected for the altitudinal gradient. It was found that the PM- ET_o calculation results were worse when the missing variable was R_s , while when VPD data were missing, the PM- ET_o estimates were closer to the PM- ET_o values calculated with the complete data set. This is evident in all statistical indicators with the lowest RMSE and the highest CE, R^2 and bR^2 . As expected, the largest error occurred when data for two variables were missing and their values were estimated (Table 6).

The site by site analysis showed that the high ET_o values were underestimated in Chirimachay, Virgen, and Toredora, and only in Chirimachay a slight overestimation of the lower values existed on PM- ET_o calculation with estimated R_s . This behavior is well explained by the relationships between R_s -DS and observed R_s as previously analyzed (Fig. 4a-o). The estimated values of PM- ET_o R_s -DS were better than R_s -DS estimates. The good relationship between PM- ET_o and PM- ET_o R_s -DS is highlighted in Fig. 6a-c and Table 6, with $R^2 > 0.82$ and $bR^2 > 78$ in the three sites. Moreover, the RMSE values were below 0.34 mm day^{-1} , and the highest performance was found in Toredora (Table 6; Fig. 6c).



The novelty of our results lies in the fact that limited information is available on this topic for humid conditions, and there is only one previous study which preliminary explored the topic in the high Tropical Andes (Córdova et al., 2015). Such investigation concluded that for the PM-ET_o calculation, the observations of R_s are extremely important in this area, because when this variable was missing, and it was estimated without local calibration, the ET_o yielded the maximum error (RMSE of 0.53 mm day⁻¹). In contrast, our results showed a decrease in the RMSE to 0.27 mm day⁻¹, after selecting the best method to estimate R_s in this zone. The research of A. P. de Souza et al. (2016) had similar findings in humid conditions in the Mato Grosso State: among the methods used to estimate R_s, the method proposed by De Jong and Stewart (1993) resulted in the lowest RMSE on PM-ET_o calculations.

Previous studies, developed under humid conditions, have reported an underestimation of high values and a slight overestimation of low values on ET_o calculation, when R_s was estimated. In this case, using the method of George H. Hargreaves and Zohrab A. Samani (1982) with the locally calibrated K_{RS} coefficient (Paredes et al., 2017; Paredes and Pereira, 2019).

On the other hand, the analysis of the results between PM-ET_o and PM-ET_o VPD-FAO indicated that when e_a data were estimated (assuming T_{dew} = T_{min} to determine VPD), the calculations had a very high performance in the altitudinal gradient. The R² values exceeded 0.96 and the bR² values exceeded 0.92. The lowest values of RMSE (< 0.19 mm day⁻¹) were supported by the high CE from 0.94 to 0.97 (Table 6). These outcomes corroborate the findings of the previous work of Córdova et al. (2015), who found that the ET_o calculation using VPD-FAO method had a RMSE of 0.17 mm day⁻¹ in Toreadora. Despite the good performance, the PM-ET_o VPD-FAO calculation showed a slight tendency to overestimate low and medium values. This finding broadly supports the work of other studies in humid conditions. For example, the work of Sentelhas et al. (2010) in Canada and Landeras et al. (2008) in Northern Spain found the ET_o was overestimated when the VPD-FAO method was applied.

As expected, the largest error occurred when both R_s-DS and VPD-FAO were used to estimate PM-ET_o instead of observations. Overall, in the altitudinal gradient, an increase in RMSE (> 0.32 mm day⁻¹) was observed, and the over and under estimation of both variables was reflected in a CE between 0.66 and 0.79. The good correlation between observed and estimated values was reflected by R² > 0.77 and bR² > 0.74 (Table 6, Fig. 6g,h,i). These findings are consistent with those of Landeras et al. (2008) in Northern



Spain, and Sentelhas et al. (2010) in Canada, with an error increment on ET_o calculation when R_s and RH data were missing.

In our study area, the estimates of R_s were less precise than VPD, and these observations were also reflected on PM- ET_o calculation. The underestimation of high ET_o values that was found when estimating R_s , was also evident in the calculation of PM- ET_o R_s -DS and VPD-FAO. Moreover, the tendency to overestimate low and medium values shown on PM- ET_o VPD-FAO calculation was also observed in the calculation of PM- ET_o R_s -DS and VPD-FAO. Despite this over- or under-estimation, the RMSE was low: 0.42, 0.32 and 0.34 mm day^{-1} for Chirimachay, Virgen, and Toreadora, respectively compared to the results reported by Córdova et al. (2015). They found a RMSE 0.71 mm day^{-1} in the Toreadora site when R_s and HR data were missing, using the recommendations of George H. Hargreaves and Zohrab A. Samani (1982) and Allen, R, (1995). Hence, the calculation of ET_o with the PM method when R_s and/or VPD were missing and were estimated with the R_s -DS and VPD-FAO methods was reliable in our study area.

Table 2

Adjustment coefficients and statistics used to evaluate the performance of the methods to estimate daily R_s in the altitudinal gradient.

Method	K_{rs}	K_{ra}	a	b	c	d	RMSE (MJ m^{-2} day^{-1})	CE	R^2	bR^2
R_s -HS	0.1094	-	-	-	-	-	3.58	0.47	0.51	0.47
R_s -DS	-	-	0.5025	0.6879	-0.0350	0.0014	3.28	0.55	0.57	0.53
R_s -AL	-	0.1376	-	-	-	-	3.58	0.47	0.51	0.47
R_s -VA	-	-	0.0045	0.1020	-	-	3.73	0.42	0.50	0.47
R_s -CH	-	-	0.1536	-0.4475	-	-	3.63	0.45	0.47	0.43

**Table 3**Statistics of the validation of the methods to estimate daily R_s in the altitudinal gradient.

Method	RMSE ($\text{MJ m}^{-2} \text{ day}^{-1}$)	CE	R^2	bR^2
R_s -HS	3.61	0.48	0.53	0.48
R_s -DS	3.42	0.53	0.54	0.50
R_s -AL	3.62	0.47	0.53	0.47
R_s -VA	3.76	0.43	0.52	0.47
R_s -CH	3.65	0.46	0.49	0.44

Table 4Statistics used to evaluate the performance of the calibrated methods for daily R_s estimation of each site.

Station	Methods	RMSE ($\text{MJ m}^{-2} \text{ day}^{-1}$)	CE	R^2	bR^2
Chirimachay	R_s -HS	3.84	0.43	0.57	0.56
	R_s -DS	3.81	0.44	0.53	0.52
	R_s -AL	3.79	0.44	0.57	0.56
	R_s -VA	4.11	0.34	0.56	0.55
	R_s -CH	3.82	0.43	0.52	0.50
Virgen	R_s -HS	3.05	0.55	0.61	0.56
	R_s -DS	2.89	0.60	0.61	0.57
	R_s -AL	3.07	0.55	0.61	0.55
	R_s -VA	3.19	0.51	0.60	0.55
	R_s -CH	3.11	0.54	0.57	0.52
Toreadora	R_s -HS	3.91	0.41	0.51	0.42
	R_s -DS	3.52	0.52	0.59	0.50
	R_s -AL	3.96	0.39	0.51	0.42
	R_s -VA	4.03	0.37	0.49	0.41
	R_s -CH	3.99	0.38	0.46	0.38

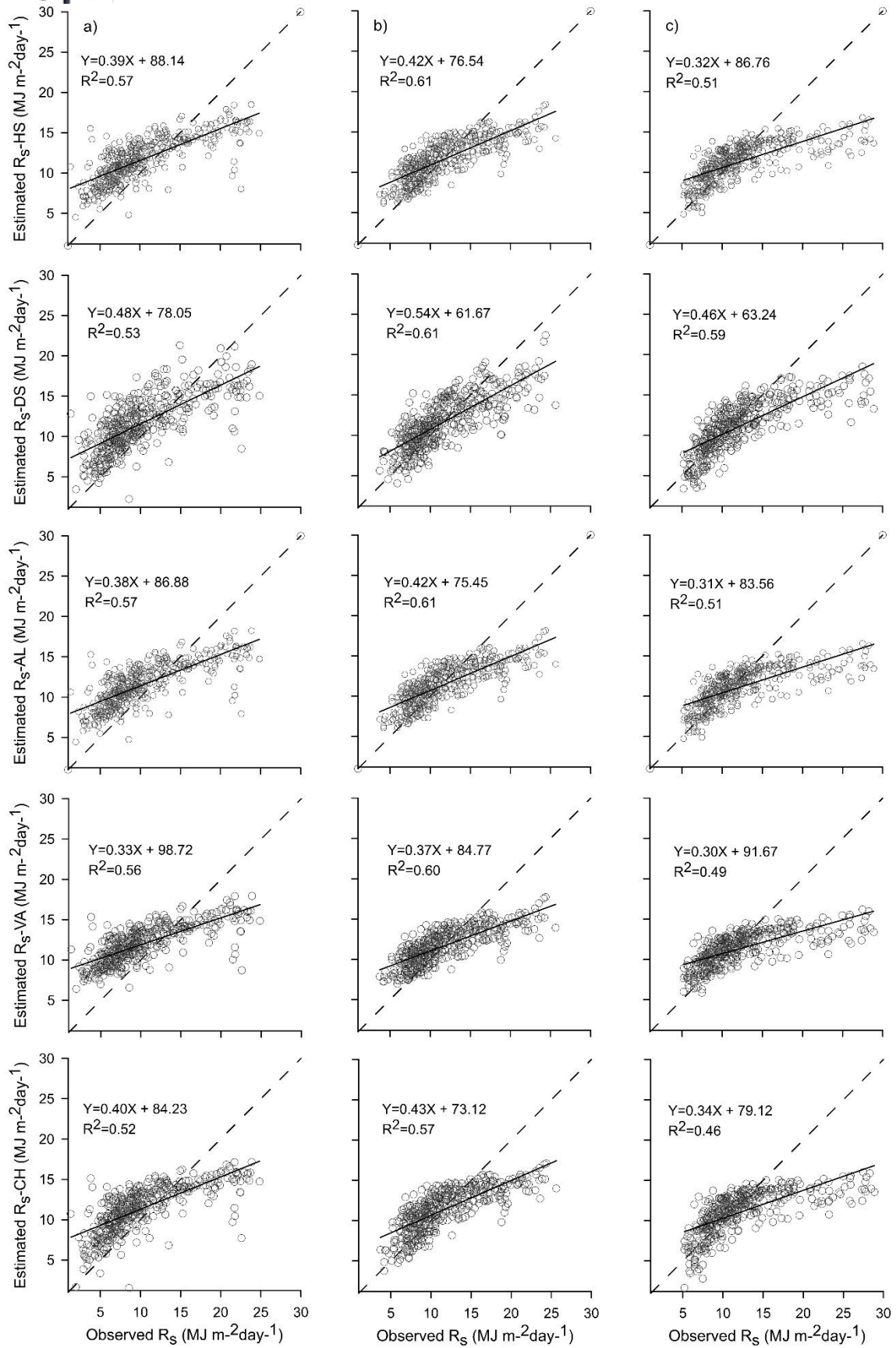




Fig. 4. Comparison of daily R_s observed and estimated (with five methods) in all stations (Chirimachay, Virgen and Toreadora). The solid line represents the fitted regression line. The dashed line indicates 1:1.

Table 5

Statistics used to evaluate the performance of the methods for daily VPD estimation of each site.

Station	Methods	RMSE (kPa)	CE	R^2	bR^2
Chirimachay	VPD-FAO	0.12	0.40	0.81	0.64
	VPD-DP	0.11	0.47	0.55	0.43
	VPD-CA1	0.30	0.32	0.58	0.43
	VPD-CA2	0.12	0.39	0.76	0.70
Virgen	VPD-FAO	0.08	0.63	0.80	0.70
	VPD-DP	0.10	0.39	0.61	0.45
	VPD-CA1	0.08	0.62	0.74	0.68
	VPD-CA2	0.1	0.30	0.79	0.62
Toreadora	VPD-FAO	0.09	0.62	0.77	0.71
	VPD-DP	0.13	0.21	0.63	0.35
	VPD-CA1	0.10	0.63	0.73	0.69
	VPD-CA2	0.13	0.24	0.75	0.59

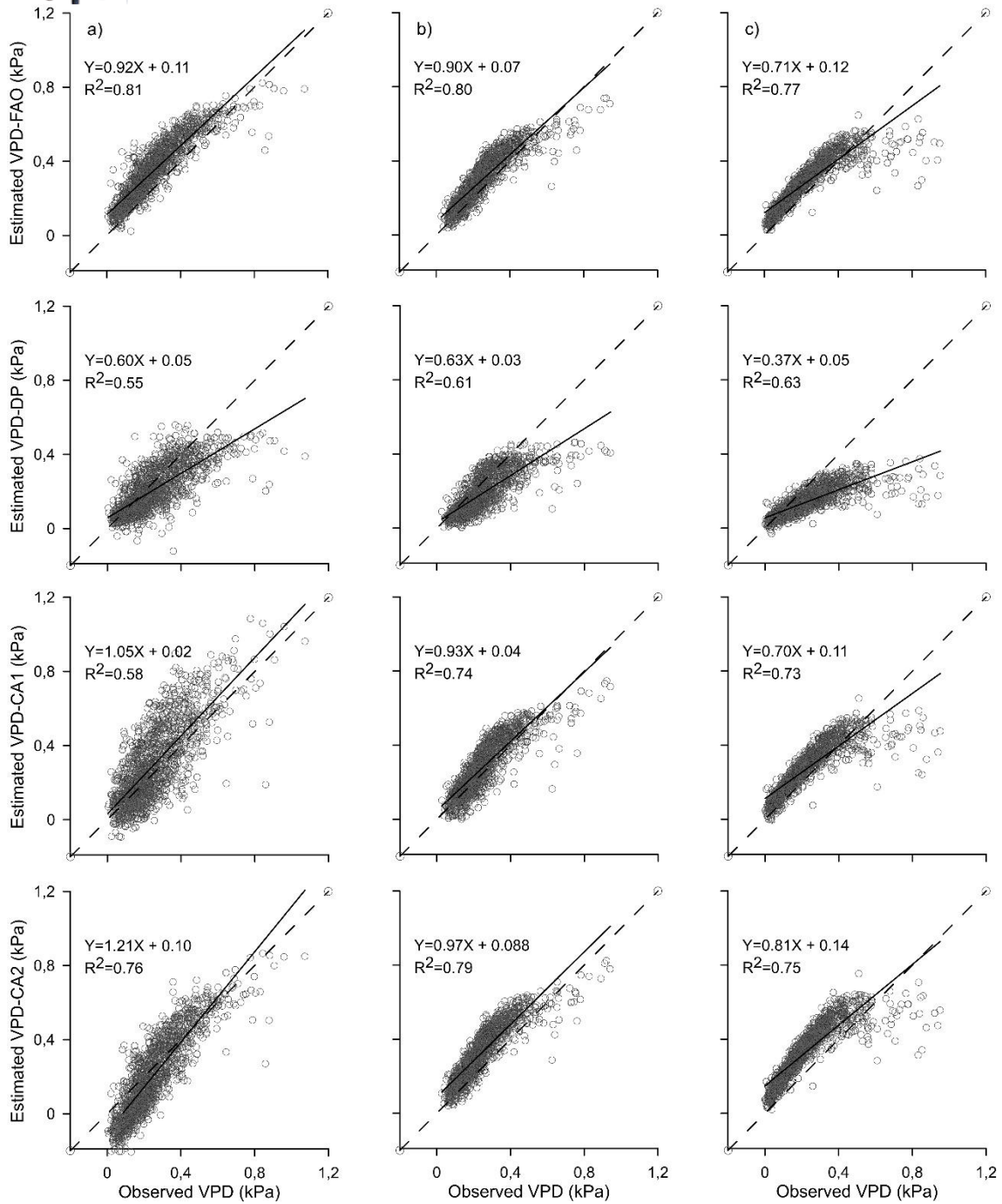


Fig. 5. Comparison of daily observed and estimated VPD (with four methods) in all stations (Chirimachay, Virgen and Toreadora). The solid line represents the fitted regression line. The dashed line indicates 1:1.

**Table 6**

Comparison between daily PM-ET_o (calculated with full data) and daily PM-ET_o (calculated when R_s and/or VPD were missing and were estimated with the best methods) (R_s-DS and VPD-FAO).

Station	ET _o	RMSE (mm day ⁻¹)	CE	R ²	bR ²
Chirimachay	R _s -DS	0.33	0.79	0.85	0.82
	VPD-FAO	0.16	0.95	0.99	0.93
	R _s -DS and VPD-FAO	0.42	0.66	0.83	0.75
Virgen	R _s -DS	0.29	0.81	0.83	0.79
	VPO-FAO	0.12	0.97	0.98	0.95
	R _s -DS and VPD-FAO	0.32	0.77	0.78	0.77
Toreadora	R _s -DS	0.27	0.86	0.89	0.83
	VPD-FAO	0.18	0.94	0.97	0.94
	R _s -DS and VPD-FAO	0.34	0.79	0.82	0.80

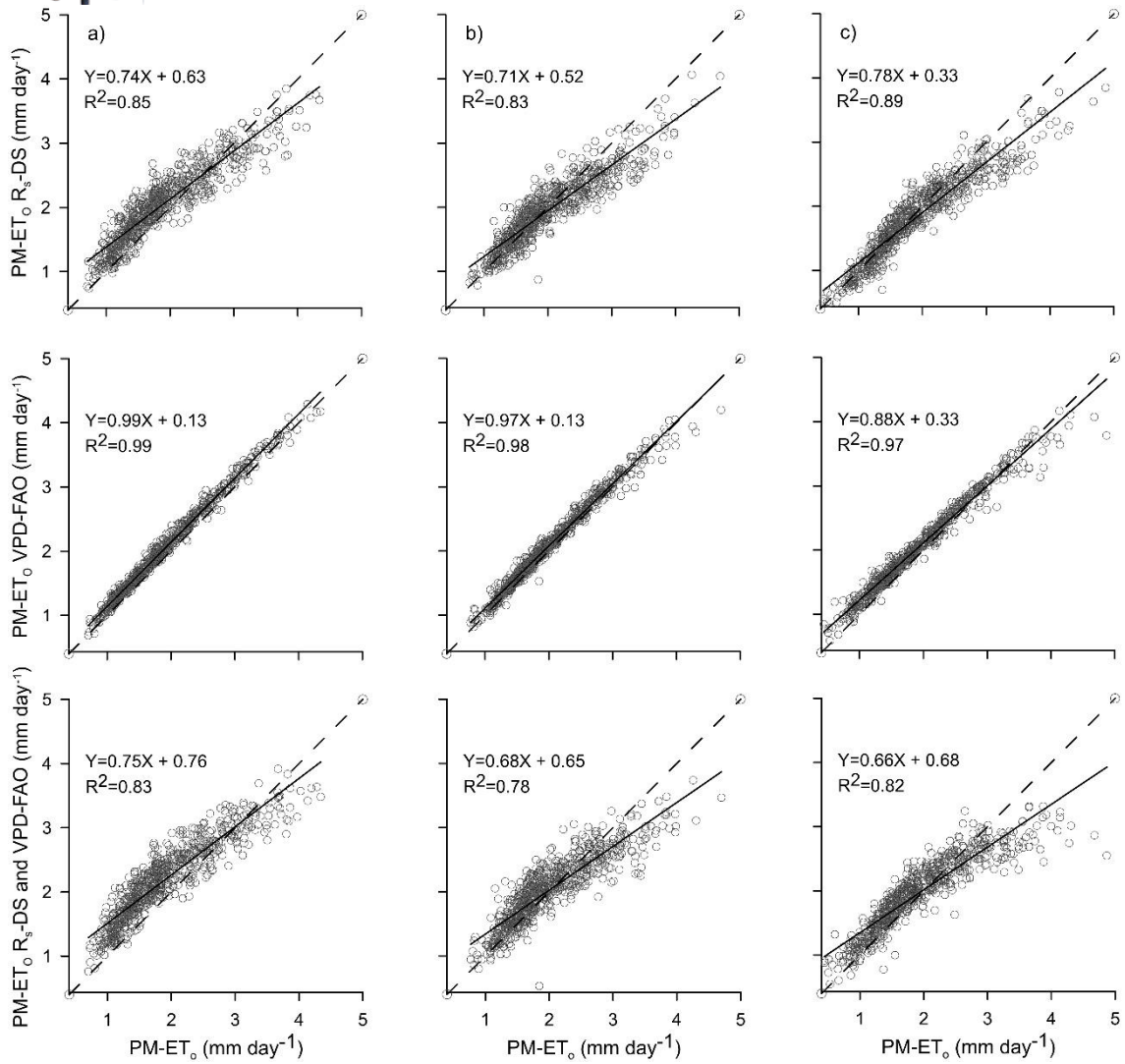


Fig. 6. Comparison of daily PM-ET₀ and PM-ET₀ R_s-DS and/or VPD-FAO in all stations: Chirimachay, Virgen and Toreadora. The solid line represents the fitted regression line. The dashed line indicates 1:1.



5 Conclusions

The objective of this investigation was to assess the impact on PM-ET_o calculation when solar radiation (R_s) and/or vapor pressure deficit (VPD) were missing in the high Tropical Andes (humid páramo, 3298 – 3955 m a.s.l.). Here, continuous high quality meteorological data are not available, or time series are incomplete. Córdova et al. (2015) proved that in the absence of observed data of R_s and relative humidity (RH), ET_o estimates are significantly affected. This study is the first in the region to evaluate nine methods to estimate R_s and VPD – based on daily maximum and minimum temperature – and to evaluate their impact on PM-ET_o calculation.

The first finding has shown that the calibration and validation of methods to calculate R_s was essential to obtain more accurate R_s estimations for this ecosystem. The De Jong and Stewart (1993) (R_s -DS) method had the highest performance in our study area, an RMSE between 2.89 and 3.81 MJ m⁻² day⁻¹ and $R^2 > 0.52$. Despite an underestimation of values above 19 MJ m⁻² day⁻¹, the R_s -DS method seems to be a feasible approach to estimate the missing variable.

The second finding has shown that the Allen et al. (1998) (VPD-FAO) method had the highest performance out of the 4 methods evaluated to estimate VPD in all statistical indicators used: RMSE between 0.08 and 0.12 kPa and $R^2 > 0.76$. Therefore, in the absence of RH observations, the use of $T_{\text{dew}} = T_{\text{min}}$ could be an excellent alternative to estimate e_a in the páramo ecosystem with a slight overestimation for low and medium values.

Finally, the results of this investigation showed that because of the fact that we properly estimated R_s and VPD, the calculation of PM-ET_o presented good statistical indicators. When only R_s is missing, PM-ET_o had an RMSE between 0.29 and 0.34 mm day⁻¹ and $R^2 > 0.82$; when only VPD is missing, PM-ET_o had an RMSE between 0.12 and 0.18 mm day⁻¹ and $R^2 > 0.96$. As expected, when both variables were missing, the ET_o calculation increased its error, an RMSE between 0.32 and 0.42 mm day⁻¹ and $R^2 > 0.77$. However, this error was much lower when compared to the results found by Córdova et al. (2015). Hence, we conclude that the calculation of ET_o with the PM method when R_s and/or VPD were missing and were estimated with the R_s -DS and VPD-FAO methods was reliable in our area.

Results obtained in the current study have shown that the calibration of equations to estimate missing variables (R_s and/or RH) provides a solution to calculate reliable PM-ET_o in the páramo ecosystem when aiming at improved water productivity for domestic



and industrial uses, irrigated agriculture, and hydropower. Moreover, the procedures herein assessed can be used for other humid locations, considering that the adjustment coefficients should be locally calibrated.

6 References

- A. P. de Souza, A. Tanaka, A. da Silva, E. Uliana, F. de Almeida, A. W. Gomes, A.K., 2016. REFERENCE EVAPOTRANSPIRATION BY PENMAN–MONTEITH FAO 56 WITH MISSING DATA OF GLOBAL RADIATION. *Brazilian J. Biosyst. Eng.* 10, 217–233. <https://doi.org/10.5151/cidi2017-060>
- Allen. R, 1995. Evaluation of procedures for estimating mean monthly solar radiation from air temperature. *J. Hydrol. Eng.* 2, 56–67.
- Allen, R.G., Pereira, L.S., Raes, D., Smith, M., Ab, W., 1998. Fao, 1998. Irrig. Drain. Pap. No. 56, FAO 300. <https://doi.org/10.1016/j.eja.2010.12.001>
- Bandyopadhyay, A., Bhadra, A., Raghuwanshi, N.S., Singh, R., 2008. Estimation of monthly solar radiation from measured air temperature extremes. *Agric. For. Meteorol.* 148, 1707–1718. <https://doi.org/10.1016/j.agrformet.2008.06.002>
- Beck, E., Bendix, J., Kottke, I., Makeschin, F., Mosandl, R., 2008. The Ecosystem (Reserva Biológica San Francisco) In: Beck, Erwin Bendix, Jörg Kottke, Ingrid Makeschin, Franz Mosandl, Reinhard Gradients in a Tropical Mountain Ecosystem of Ecuador. *Ecological Studies*, 198.
- Bennett, N.D., Croke, B.F., Guariso, G., Guillaume, J.H., Hamilton, S.H., Jakeman, A.J., Marsili-Libelli, S., Newham, L.T., Norton, J.P., Perrin, C., Pierce, S.A., Robson, B., Seppelt, R., Voinov, A.A., Fath, B.D., Andreassian, V., Land, C., 2013. Characterising performance of environmental models q. *Environ. Model. Softw.* 40, 1–20. <https://doi.org/10.1016/j.envsoft.2012.09.011>
- Besharat, F., Dehghan, A.A., Faghieh, A.R., 2013. Empirical models for estimating global solar radiation: A review and case study. *Renew. Sustain. Energy Rev.* 21, 798–821. <https://doi.org/10.1016/j.rser.2012.12.043>
- Buytaert, W., Céleri, R., De Bièvre, B., Cisneros, F., Wyseure, G., Deckers, J., Hofstede, R., 2006. Human impact on the hydrology of the Andean páramos. *Earth-Science Rev.* 79, 53–72. <https://doi.org/10.1016/j.earscirev.2006.06.002>
- Carrillo-Rojas, G., Silva, B., Córdova, M., Céleri, R., Bendix, J., 2016. Dynamic mapping of evapotranspiration using an energy balance-based model over an andean páramo catchment of southern ecuador. *Remote Sens.* 8. <https://doi.org/10.3390/rs8020160>
- Castellví, F., Perez, P.J., Stockle, C.O., Ibañez, M., 1997. Methods for estimating vapor pressure deficit at a regional scale depending on data availability. *Agric. For. Meteorol.* 87, 243–252. [https://doi.org/10.1016/S0168-1923\(97\)00034-8](https://doi.org/10.1016/S0168-1923(97)00034-8)
- Céleri, R., Feyen, J., 2009. The Hydrology of Tropical Andean Ecosystems: Importance, Knowledge Status, and Perspectives. *Mt. Res. Dev.* 29, 350–355. <https://doi.org/10.1659/mrd.00007>
- Chen, R., Ersi, K., Yang, J., Lu, S., Zhao, W., 2004. Validation of five global radiation



- models with measured daily data in China. *Energy Convers. Manag.* 45, 1759–1769. <https://doi.org/10.1016/j.enconman.2003.09.019>
- Córdova, M., Carrillo-Rojas, G., Crespo, P., Wilcox, B., Céleri, R., 2015. Evaluation of the Penman-Monteith (FAO 56 PM) Method for Calculating Reference Evapotranspiration Using Limited Data. *Mt. Res. Dev.* 35, 230. <https://doi.org/10.1659/mrd-journal-d-14-0024.1>
- da Silva, G.H., Dias, S.H.B., Ferreira, L.B., Santos, J.É.O., da Cunha, F.F., 2018. Performance of different methods for reference evapotranspiration estimation in Jaíba, Brazil. *Rev. Bras. Eng. Agric. e Ambient.* 22, 83–89. <https://doi.org/10.1590/1807-1929/agriambi.v22n2p83-89>
- De Jong, R., Stewart, D.W., 1993. Estimating global solar radiation from common meteorological observations in western Canada. *Can. J. Plant Sci.* 73, 509–518. <https://doi.org/10.4141/cjps93-068>
- Doorenbos, J., Pruitt, W.O., 1977. Guidelines for predicting crop water requirements. *FAO Irrig. Drain. Pap.* 24, 144.
- Garreaud, R.D., 2009. The Andes climate and weather. *Adv. Geosci.* 22, 3–11. <https://doi.org/10.5194/adgeo-22-3-2009>
- George H. Hargreaves, Zohrab A. Samani, 1982. Estimating Potential Evapotranspiration. *J. Irrig. Drain. Div.* 108, 225–230.
- Jabloun, M., Sahli, A., 2008. Evaluation of FAO-56 methodology for estimating reference evapotranspiration using limited climatic data. Application to Tunisia. *Agric. Water Manag.* 95, 707–715. <https://doi.org/10.1016/j.agwat.2008.01.009>
- Karimi, S., Shiri, J., Marti, P., 2020. Supplanting missing climatic inputs in classical and random forest models for estimating reference evapotranspiration in humid coastal areas of Iran. *Comput. Electron. Agric.* 176, 105633. <https://doi.org/10.1016/j.compag.2020.105633>
- Landeras, G., Ortiz-Barredo, A., López, J.J., 2008. Comparison of artificial neural network models and empirical and semi-empirical equations for daily reference evapotranspiration estimation in the Basque Country (Northern Spain). *Agric. Water Manag.* 95, 553–565. <https://doi.org/10.1016/j.agwat.2007.12.011>
- Li, H., Cao, F., Wang, X., Ma, W., 2014. A temperature-based model for estimating monthly average daily global solar radiation in China. *Sci. World J.* 2014. <https://doi.org/10.1155/2014/128754>
- Li, M.F., Fan, L., Liu, H. Bin, Guo, P.T., Wu, W., 2013. A general model for estimation of daily global solar radiation using air temperatures and site geographic parameters in Southwest China. *J. Atmos. Solar-Terrestrial Phys.* 92, 145–150. <https://doi.org/10.1016/j.jastp.2012.11.001>
- Liu, X., Mei, X., Li, Y., Wang, Q., Jensen, J.R., Zhang, Y., Porter, J.R., 2009. Evaluation of temperature-based global solar radiation models in China. *Agric. For. Meteorol.* 149, 1433–1446. <https://doi.org/10.1016/j.agrformet.2009.03.012>
- Llambí, L.D., Soto, A., Céleri, R., De Bievre, B., Ochoa, B., Borja, P., 2012. *Ecología, Hidrología y Suelos de Páramos. Proy. Páramo Andin.* 284.
- Ministerio de Agricultura y Ganadería, M., Instituto Interamericano de Cooperación para la Agricultura, I., Gobiernos Autónomos Descentralizados Provinciales, CONGOPE, C. de G.A.P. del E., DHSA, D.H. de la S. del A., OG, O. de R., Foro de los Recursos Hídricos, F., 2019. Plan Nacional de Riego y Drenaje.



- Motavita, D.F., Chow, R., Guthke, A., Nowak, W., 2019. The comprehensive differential split-sample test: A stress-test for hydrological model robustness under climate variability. *J. Hydrol.* 573, 501–515. <https://doi.org/10.1016/j.jhydrol.2019.03.054>
- Ochoa-Sánchez, A., Crespo, P., Carrillo-Rojas, G., Sucozhañay, A., Célleri, R., 2019. Actual evapotranspiration in the high andean grasslands: A comparison of measurement and estimation methods. *Front. Earth Sci.* 7, 1–16. <https://doi.org/10.3389/feart.2019.00055>
- Paredes, P., Fontes, J.C., Azevedo, E.B., Pereira, L.S., 2017. Daily reference crop evapotranspiration with reduced data sets in the humid environments of Azores islands using estimates of actual vapor pressure, solar radiation, and wind speed. *Theor. Appl. Climatol.* 134, 1115–1133. <https://doi.org/10.1007/s00704-017-2329-9>
- Paredes, P., Pereira, L.S., 2019. Computing FAO56 reference grass evapotranspiration PM-ET o from temperature with focus on solar radiation. *Agric. Water Manag.* 215, 86–102. <https://doi.org/10.1016/j.agwat.2018.12.014>
- Paredes, P., Pereira, L.S., Almorox, J., Darouich, H., 2020. Reference grass evapotranspiration with reduced data sets: Parameterization of the FAO Penman-Monteith temperature approach and the Hargeaves-Samani equation using local climatic variables. *Agric. Water Manag.* 240, 106210. <https://doi.org/10.1016/j.agwat.2020.106210>
- Perrin, C., Oudin, L., Andreassian, V., Rojas-Serna, C., Michel, C., Mathevet, T., 2007. Impact of limited streamflow data on the efficiency and the parameters of rainfall-runoff models. *Hydrol. Sci. J.* 52, 131–151. <https://doi.org/10.1623/hysj.52.1.131>
- R. Hofstede, J. Calles, V. López, R. Polanco, F. Torres, J. Ulloa, A. Vásquez, M.C., 2014. LOS PÁRAMOS ANDINOS ¿Qué Sabemos? Estado de conocimiento sobre el impacto del cambio climático en el ecosistema páramo. UICN, Quito, Ecuador 7–61. <https://doi.org/10.2307/j.ctvpv50bh.8>
- Raziei, T., Pereira, L.S., 2013. Estimation of ETo with Hargreaves-Samani and FAO-PM temperature methods for a wide range of climates in Iran. *Agric. Water Manag.* 121, 1–18. <https://doi.org/10.1016/j.agwat.2012.12.019>
- Ren, X., Qu, Z., Martins, D.S., Paredes, P., Pereira, L.S., 2016. Daily Reference Evapotranspiration for Hyper-Arid to Moist Sub-Humid Climates in Inner Mongolia, China: I. Assessing Temperature Methods and Spatial Variability. *Water Resour. Manag.* 30, 3769–3791. <https://doi.org/10.1007/s11269-016-1384-9>
- Samani, Z., 2000. Estimación de la Evapotranspiración y la Radiación Solar usando un mínimo de datos climáticos. *J. Irrig. Drain. Eng.* 126, 265–267.
- Santos, J.E.O., Cunha, F.F. da, Filgueiras, R., Silva, G.H. da, Castro Teixeira, A.H. de, Santos Silva, F.C. dos, Sedyama, G.C., 2020. Performance of SAFER evapotranspiration using missing meteorological data. *Agric. Water Manag.* 233, 106076. <https://doi.org/10.1016/j.agwat.2020.106076>
- Sentelhas, P.C., Gillespie, T.J., Santos, E.A., 2010. Evaluation of FAO Penman-Monteith and alternative methods for estimating reference evapotranspiration with missing data in Southern Ontario, Canada. *Agric. Water Manag.* 97, 635–644. <https://doi.org/10.1016/j.agwat.2009.12.001>
- Tabari, H., Hosseinzadehtalaei, P., Willems, P., Martinez, C., 2016. Validation and calibration of solar radiation equations for estimating daily reference evapotranspiration at cool semi-arid and arid locations. *Hydrol. Sci. J.* 61, 610–619. <https://doi.org/10.1080/02626667.2014.947293>



- Todorovic, M., Karic, B., Pereira, L.S., 2013. Reference evapotranspiration estimate with limited weather data across a range of Mediterranean climates. *J. Hydrol.* 481, 166–176. <https://doi.org/10.1016/j.jhydrol.2012.12.034>
- Tomas-Burguera, M., Vicente-Serrano, S.M., Grimalt, M., Beguería, S., 2017. Accuracy of reference evapotranspiration (ET_o) estimates under data scarcity scenarios in the Iberian Peninsula. *Agric. Water Manag.* 182, 103–116. <https://doi.org/10.1016/j.agwat.2016.12.013>
- Vanderlinden, K., Giráldez, J. V., Van Meirvenne, M., 2004. Assessing Reference Evapotranspiration by the Hargreaves Method in Southern Spain. *J. Irrig. Drain. Eng.* 130, 184–191. [https://doi.org/10.1061/\(ASCE\)0733-9437\(2004\)130:3\(184\)](https://doi.org/10.1061/(ASCE)0733-9437(2004)130:3(184))
- Wright, C., Kagawa-Viviani, A., Gerlein-Safdi, C., Mosquera, G.M., Poca, M., Tseng, H., Chun, K.P., 2018. Advancing ecohydrology in the changing tropics: Perspectives from early career scientists. *Ecohydrology* 11. <https://doi.org/10.1002/eco.1918>
- Xia, Y., Yang, Z.L., Jackson, C., Stoffa, P.L., Sen, M.K., 2004. Impacts of data length on optimal parameter and uncertainty estimation of a land surface model. *J. Geophys. Res. D Atmos.* 109. <https://doi.org/10.1029/2003jd004419>

Appendix A

Table A1



Details of the sensors.

Variable	Sensor Type	Unit	Accuracy	Time Resolution
Air temperature / Relative Humidity	Campbell CS-215 + Radiation Shield	°C/%RH	±0.3°C/±2% RH	5 min
Solar Radiation	Campbell CS300 Pyranometer	W m ⁻²	± 5% daily total	5 min
Wind Speed and Direction	Met-One 034B Wind Set	m s ⁻¹	± 0.11 m s ⁻¹	5 min

Table A2

Range of the adjustable coefficients of each method.

Methods	K _{rs}	K _{ra}	a	b	c	d
R _s -HS	0.096-0.12	-	-	-	-	-
R _s -DS	-	-	0.48-0.52	0.65-0.80	-0.03-0.017	0.0009-0.004
R _s -AL	-	0.10-0.15	-	-	-	-
R _s -VA	-	-	0.045-0.1	0.01-0.03	-	-
R _s -CH	-	-	0.149-0.159	-0.47-0.3	-	-

Table A3

Performance evaluation criteria.

Criteria	Equation	Optimal value
Nash–Sutcliffe efficiency	$CE = 1 - \frac{\sum_{i=1}^n (x_i - x_o)}{\sum_{i=1}^n (x_o - \underline{x_o})}$	1
Coefficient of determination	$R^2 = \frac{\sum_{i=1}^n (x_i - \underline{x_o})^2}{\sum_{i=1}^n (x_o - \underline{x_o})^2}$	1
Coefficient of determination multiplied by the slope	$br^2 = b R^2, b \leq 1; br^2 = \frac{R^2}{ b }, b > 1$	1
Root mean square error	$RMSE = \sqrt{\frac{1}{n} \sum_{i=1}^n (x_i - x_o)^2}$	0

Where x_i is the estimated value; x_o is the observed value; n is the number of observations and $\underline{x_o}$ is the mean of the observed values.